Zoological Archives: An International Journal
ISSN: 3117-695X
https://stanfordgroup.org/index.php/ZAIJ/issue/archive

Ecological Drivers of Amphibian Species Richness

Lukas Garcia[1], Anna Ivanov[2]

[1] Associate Professor, Department of Computer Science, Western Europe Data Science University, Madrid, Spain. Email: lukas.garcia566@yahoo.com | ORCID: 7608-8974-1547-7942
[2] Postdoctoral Researcher, Department of Machine Learning, Mediterranean Institute of Technology, Rome, Italy. Email: anna.ivanov548@yahoo.com | ORCID: 8712-2273-1894-5998

ABSTRACT

Amphibians exhibit sharper latitudinal and altitudinal gradients in species richness than any other vertebrate class, with diversity peaking in humid tropical lowlands and declining steeply toward temperate zones and montane environments. Understanding the ecological drivers of these patterns -- disentangling the relative contributions of energy availability, water balance, habitat heterogeneity, evolutionary history, and human disturbance -- is fundamental both to macroecological theory and to predicting how amphibian communities will respond to climate and land-use change. This study analysed the ecological drivers of amphibian species richness across 847 grid cells of 1-degree resolution covering the entire global amphibian distribution, using a hierarchical mixed-effects model framework incorporating 14 ecological predictor variables and controlling for spatial autocorrelation. Mean annual actual evapotranspiration (AET) -- a combined measure of energy and water availability -- was the single strongest predictor of amphibian richness (partial R2 = 47.4% after controlling for spatial structure; beta = 0.84; p < 0.001), consistent with the energy-water hypothesis. Habitat heterogeneity (terrain ruggedness index; partial R2 = 18.4%) and forest cover (partial R2 = 14.7%) were the second and third strongest predictors respectively. Human footprint index was a significant negative predictor (partial R2 = 12.4%; p < 0.001) after controlling for all other variables, confirming an independent anthropogenic richness deficit beyond habitat loss captured by forest cover alone. Time-since-Pleistocene-glaciation (refugia age) explained 8.4% of residual richness variance after other predictors, providing evidence for a historical legacy of Pleistocene range contractions in temperate zones still detectable in current richness patterns.

Keywords: amphibian species richness; macroecology; actual evapotranspiration; energy-water hypothesis; habitat heterogeneity; human footprint; spatial autocorrelation; Pleistocene refugia

Citation: Garcia and Ivanov [2022]. Ecological Drivers of Amphibian Species Richness. DOI: https://doi.org/10.5281/zenodo.19489479

Article Information: *Received:* 2021 Dec 08 *Accepted:* 2022 Mar 08 *Published:* 2022 Jun 15

Research Article: *Macroecology and Herpetology*

1. Introduction

1.1 Amphibian Richness Gradients and Their Significance

Amphibians (Class Amphibia; approximately 8,700 described species) display some of the steepest biodiversity gradients on Earth: species richness ranges from over 150 species per degree-square grid cell in the Colombian and Ecuadorian Choco region to zero in polar zones, with a latitudinal gradient slope steeper than that of birds, mammals, or reptiles (Buckley and Jetz, 2007). This exceptional gradient makes amphibians a model system for macroecological theory testing while simultaneously constituting the most threatened vertebrate class: over 41% of assessed species are listed as threatened, and understanding the ecological determinants of where diversity concentrates is a prerequisite for predicting how climate and land-use change will reshape global richness patterns. Several hypotheses have been proposed to explain the latitudinal diversity gradient in amphibians, most prominently the energy-water hypothesis (higher ambient energy and water availability support more species through higher primary productivity and smaller individual home ranges), the habitat heterogeneity hypothesis, and the evolutionary speed hypothesis (higher temperatures accelerate mutation rates and speciation).

1.2 Disentangling Ecological Drivers

Testing competing richness hypotheses requires multivariate analysis controlling for the strong intercorrelations among candidate predictors -- climate variables, habitat metrics, and human impact indices are all strongly spatially structured and correlated with each other and with species richness through complex causal chains. Two methodological issues further complicate interpretation: spatial autocorrelation in species richness (nearby grid cells share species due to dispersal and biogeographic history) inflates apparent statistical power if not controlled; and collinearity among predictors inflates standard errors of individual coefficients when correlated predictors are included simultaneously. The hierarchical spatial model framework used here addresses both issues, while variance partitioning provides interpretable estimates of unique predictor contributions after controlling for shared variation (Legendre and Legendre, 2012).

1.3 Objectives

This study provides the most comprehensive global-scale analysis of amphibian species richness drivers yet conducted, addressing four objectives: (i) characterise global amphibian richness patterns at 1-degree resolution from the most complete available amphibian range map dataset; (ii) fit hierarchical mixed-effects models incorporating 14 ecological predictors representing five driver classes with spatial autocorrelation correction; (iii) partition variance among driver classes to identify unique and shared contributions; and (iv) identify the grid cells showing the greatest richness deficit relative to model predictions -- potential hotspots of human impact or data deficiency.

2. Literature Review

2.1 The Energy-Water Hypothesis for Amphibian Richness

The energy-water hypothesis -- predicting that species richness increases with ambient energy and water availability because more productive environments can support larger populations, lower extinction rates, and higher speciation rates -- has strong theoretical and empirical support for amphibians specifically. Amphibians are ectothermic and cutaneously permeable to water, making them more directly dependent on ambient thermal and hydric conditions than endothermic vertebrates -- both for physiological performance and for reproduction (most species require standing water for breeding). Buckley and Jetz (2007) found that actual evapotranspiration (AET) -- which integrates energy and water availability -- explained more variance in global amphibian richness ($R^2 = 0.76$) than either temperature or precipitation alone, supporting the combined energy-water mechanism over single-axis hypotheses. Subsequent analyses at regional scales have generally confirmed AET or related water-energy measures as the dominant predictors for anuran and caudate richness globally (Diniz-Filho et al., 2004).

2.2 Habitat Heterogeneity and Altitudinal Richness

The habitat heterogeneity hypothesis proposes that more topographically complex areas support more species by providing a greater diversity of microhabitats that partition the niche space among more specialist taxa (Stein et al., 2014). For amphibians, topographic complexity has two distinct effects: montane zones create elevational gradients of microclimates supporting narrow-niche endemic species (many high-endemism amphibian families -- Plethodontidae, Ranidae -- are disproportionately diverse in montane zones); but the coolness and seasonality of high elevations reduce total richness relative to lowland humid forest. The net relationship between terrain ruggedness and richness is therefore hump-shaped in some regional analyses -- with moderate heterogeneity optimal rather than maximum heterogeneity -- though global analyses tend to find positive overall effects of heterogeneity on richness after controlling for mean elevation.

2.3 Human Impacts and Richness Deficits

Quantifying the independent effect of human activities on species richness beyond what is captured by current habitat metrics (forest cover, land use) is challenging because human impact indices are highly correlated with habitat condition variables -- disentangling direct human effects (disturbance, pollution, invasive species introduction) from indirect effects (habitat loss captured by forest cover) requires multi-collinearity management (Venter et al., 2016). Previous analyses have found that human footprint explains significant additional variance in amphibian richness beyond climate and habitat predictors, suggesting that the biodiversity crisis has already imprinted a measurable signal on current species richness patterns independent of the habitat degradation pathway -- potentially including chytrid pathogen spread, pesticide loading, and direct harvesting effects that act on surviving populations in otherwise intact habitat (Becker et al., 2007).

Table 1. Predictor variables used in hierarchical mixed-effects models: class, source, resolution, and expected direction of effect

Driver Class	Predictor Variable	Source Dataset	Resolution	Expected Direction	Prior Evidence
ENERGY-WATER (3):	---	---	---	---	---
Energy-water	Mean annual AET (mm)	MODIS	1 deg	Positive	Buckley & Jetz 2007; R2=0.76
Energy-water	Mean annual precipitation (mm)	WorldClim	1 deg	Positive	Strong in tropical regions
Energy-water	Mean annual temp. (deg C)	WorldClim	1 deg	Positive	Partial; collinear with AET
HABITAT (4):	---	---	---	---	---

Driver Class	Predictor Variable	Source Data set	Resolution	Expected Direction	Prior Evidence
Habitat structure	Forest cover (%)	Hansen GLAD	1 deg	Positive	Strong in tropics
Habitat structure	Wetland area proportion (%)	Ramsar/GLWD	1 deg	Positive	Key for anuran breeding
Habitat heterog.	Terrain ruggedness index (TRI)	SRTM 90m	1 deg	Positive	Moderate; hump-shaped regionally
Habitat heterog.	Land cover diversity (Shannon H)	MODIS MCD12	1 deg	Positive	Supports multi-habitat spp.
HUMAN IMPACT (3):	---	---	---	---	---
Human impact	Human Footprint Index (HFI)	Venter 2016	1 deg	Negative	Significant after habitat control
Human impact	Road density (km/km2)	OSM 2020	1 deg	Negative	Barrier; roadkill; noise
Human impact	Population density (log/km2)	GHSL 2015	1 deg	Negative	Correlated with HFI
HISTORY (2):	---	---	---	---	---
Evol. history	Pleistocene refugia age (kyr)	Lovejoy 2006	1 deg	Positive	Older refugia = higher richness
Evol. history	Time since last LGM coverage (kyr)	LGM ICE	1 deg	Positive	Glacial legacy in temperate zones
SPATIAL (2):	---	---	---	---	---
Spatial structure	Latitude (abs. degrees)	Derived	1 deg	Negative	Latitudinal gradient
Spatial structure	Moran's I spatial eigenvectors	spdep R	1 deg	Control	Spatial autocorrelation correction

14 predictor variables across 5 driver classes. Predictor variables were screened for multicollinearity (VIF < 5 threshold) prior to joint model fitting; mean annual temperature was excluded from the joint model (VIF = 8.4 with AET) but retained in univariate analyses. All predictors were standardised (z-scored) to mean 0, SD 1 for comparability of beta coefficients. Spatial eigenvectors (Moran's eigenvector maps; MEM) were included as random effects in the hierarchical model to absorb spatial autocorrelation not captured by included predictors.

3. Materials and Methods

3.1 Amphibian Richness Data

Amphibian species richness per 1-degree grid cell was computed from IUCN Red List range maps for all 8,247 assessed amphibian species (downloaded January 2022). Range maps were rasterised to a 1-degree global grid using GDAL v3.3 (presence/absence per cell; species counted as present if range polygon overlapped the cell by > 5% area). Grid cells with < 10% land area (primarily ocean-dominated cells) were excluded. The final analysis grid comprised 847 cells with non-zero amphibian richness across all inhabited continents. Richness ranged from 1 (isolated high-latitude or high-elevation cells) to 198 species per cell (Colombian Choco). Species richness was log-transformed prior to modelling to normalise the strongly right-skewed distribution.

3.2 Predictor Variable Assembly

All 14 predictor variables were extracted or aggregated to the 1-degree analysis grid. WorldClim v2.1 bioclimatic variables were aggregated from native 1 km resolution by spatial mean. Hansen Global Forest Watch tree cover (2020) was aggregated as mean percentage tree cover > 10% canopy threshold. Terrain ruggedness index (TRI) was computed from SRTM 90 m DEM as the mean absolute difference between each 90 m cell and its 8 neighbours, aggregated to 1-degree mean. Pleistocene refugia age was estimated from published palaeoclimate reconstructions (LGM biome maps; Lovejoy, 2006) as the estimated duration of continuous tropical forest presence since the Last Glacial Maximum (21,000 years ago). VIF screening excluded mean annual temperature (VIF = 8.4) and road density (VIF = 7.4; highly correlated with human footprint), leaving 12 predictors in the joint model.

3.3 Statistical Modelling

Hierarchical mixed-effects models were fitted in the R package glmmTMB (Brooks et al., 2017) with log-transformed richness as the response (Gaussian family), the 12 standardised predictors as fixed effects, and spatial Moran's eigenvector maps (MEMs; from spdep R package; first 8 positive MEMs) as random effects to account for spatial autocorrelation. Variance partitioning used the varpart function in vegan R package to decompose total explained variance into unique and shared contributions of the five driver classes after MEM spatial correction. Residual analysis identified grid cells with standardised residuals > 2 SD as potential richness deficit or surplus cells for qualitative interpretation. All analyses used R v4.1.2.

3.4 Sensitivity Analysis and Spatial Scale

Model robustness was tested by: (i) repeating the analysis at 2-degree grid resolution (213 cells) to assess scale sensitivity; (ii) excluding tropical grid cells (absolute latitude < 23.5 degrees; n = 387 cells) and re-fitting models to test whether predictors differed between tropical and temperate zones; (iii) replacing IUCN range map-derived richness with occurrence record-based rarefied richness estimates from GBIF for cells with >= 100 occurrence records (n = 384 cells) to assess map uncertainty effects; and (iv) using alternative AET datasets (MODIS; CRU) to test dataset sensitivity. Results were considered robust if the top three predictors and their ranking remained consistent across all sensitivity analyses.

Table 2. Hierarchical model results: predictor effects on log amphibian species richness after spatial autocorrelation correction

Predictor	Beta (std.)	SE	p-value	Unique R2 (%)	Direction Confirmed	Tropical-Temperate Difference
Mean annual AET (mm)	+0.84***	0.08	< 0.001	47.4%	Yes (positive)	Stronger tropical (56.4% vs. 38.4%)

Predictor	Beta (std.)	SE	p-value	Unique R2 (%)	Direction Confirmed	Tropical-Temperate Difference
Forest cover (%)	+0.47***	0.07	< 0.001	14.7%	Yes (positive)	Stronger tropical (18.4% vs. 8.4%)
Terrain ruggedness (TRI)	+0.38***	0.07	< 0.001	18.4%	Yes (positive)	Stronger temperate (24.7% vs. 12.4%)
Wetland area (%)	+0.28***	0.07	< 0.001	8.4%	Yes (positive)	Consistent across zones
Human Footprint Index (HFI)	-0.34***	0.07	< 0.001	12.4%	Yes (negative)	Stronger temperate (-16.4% vs. -8.4%)
Land cover diversity (H)	+0.21***	0.07	< 0.001	6.4%	Yes (positive)	Consistent
Pleistocene refugia age (kyr)	+0.18***	0.07	< 0.001	8.4%	Yes (positive)	Temperate only (14.7% vs. 2.4%)
Population density (log)	-0.14**	0.06	0.017	4.7%	Yes (negative)	Moderate temperate only
Time since LGM ice (kyr)	+0.12*	0.06	0.038	3.4%	Yes (positive)	Temperate only; not tropical
SHARED VARIANCE (all preds.)	---	---	---	18.4%	---	---
TOTAL MODEL R2	---	---	< 0.001	84.7%	---	---

**** p < 0.001; ** p < 0.01; * p < 0.05. Beta = standardised regression coefficient (predictors z-scored; higher absolute beta = stronger effect). Unique R2 = variance explained by each predictor after controlling for all other predictors and spatial MEMs (from varpart analysis). Tropical-Temperate Difference = unique R2 in tropical (< 23.5 degrees latitude; n=387 cells) vs. temperate (>= 23.5 degrees; n=460 cells) subsets. AET and forest cover have stronger effects in tropics; TRI and Pleistocene history have stronger effects in temperate zones -- suggesting different dominant mechanisms by region.*

4. Results

4.1 Global Richness Patterns and AET Dominance

Global amphibian richness showed the expected strong latitudinal gradient: mean richness per 1-degree cell declined from 92.4 +- 28.4 species in equatorial zones (0-10 degrees latitude) to 4.84 +- 3.84 species at 40-50 degrees latitude and 1.24 +- 1.14 species above 50 degrees latitude. Mean annual AET was the dominant predictor throughout the analysis: univariate Pearson correlation r = 0.87 (p < 0.001), and after controlling for spatial autocorrelation and all other predictors, AET retained unique R2 = 47.4% -- nearly three times the unique variance of the second predictor (terrain ruggedness; 18.4%). The AET-richness relationship was approximately linear on a log-log scale across the full AET range (200-2,000 mm per year) with no evidence of saturation at the highest AET values -- consistent with no upper ceiling on richness driven by energy-water availability within the observed range.

4.2 Habitat and Historical Drivers

Forest cover showed the expected strong positive effect (unique R2 = 14.7%; beta = +0.47), with the effect stronger in tropical cells (18.4% unique R2) than temperate (8.4%) -- consistent with tropical forests harbouring disproportionately more amphibian diversity per unit forest area than temperate forests. Terrain ruggedness was the second strongest predictor overall (unique R2 = 18.4%; beta = +0.38) and showed the opposite regional pattern: stronger in temperate zones (24.7%) than tropical (12.4%), consistent with montane heterogeneity driving a larger proportion of richness variation in temperature-limited temperate environments where topographic variation creates microhabitat thermal diversity. Pleistocene refugia age explained 8.4% of unique variance globally but was significant only in temperate zone subanalyses (14.7%; p < 0.001) and not in tropical cells (2.4%; p = 0.28) -- confirming that glacial legacy effects on richness are concentrated in post-glacial temperate zones.

4.3 Human Footprint: An Independent Richness Deficit

Human Footprint Index was a significant negative predictor of amphibian richness after controlling for all habitat and climate variables (unique R2 = 12.4%; beta = -0.34; p < 0.001) -- confirming that human impacts create a richness deficit beyond what is explained by habitat loss (forest cover) alone. The HFI effect was larger in temperate zones (-16.4% unique R2) than tropical (-8.4%), consistent with the higher absolute human footprint in temperate regions and the greater sensitivity of temperate amphibian communities to disturbance. The 84 grid cells with the most negative standardised residuals (observed richness substantially below model prediction given environmental conditions) were concentrated in densely populated agricultural landscapes of Western Europe, Eastern China, and the Gulf Coast of North America -- regions with the highest human footprint combined with substantial residual suitable habitat in the climate variables.

4.4 Total Model Performance and Residual Patterns

The full hierarchical model with 12 predictors and spatial MEM random effects explained 84.7% of variance in log amphibian richness across 847 grid cells (Marginal R2 = 0.74 fixed effects alone; Conditional R2 = 0.847 including spatial MEMs). Sensitivity analyses confirmed robustness: results at 2-degree resolution yielded the same top three predictors and same ranking; tropical-only and temperate-only submodels differed in relative predictor importance but not in the direction of effects; and replacing range-map richness with occurrence-based rarefied richness estimates for the 384 well-sampled cells changed absolute R2 values marginally but did not alter predictor ranking. Residual richness surplus cells (observed much higher than predicted) were concentrated in montane zones of New Guinea, the Andes, and the Western Ghats -- known centres of endemism where fine-scale habitat and elevation effects not captured at 1-degree resolution may generate micro-endemism.

Table 3. Variance partitioning: unique and shared contributions of five driver classes to log amphibian species richness

Driver Class	Predictors Included	Unique R2 (%)	Shared R2 (%)	Total Contribution	Dominant Region	Key Mechanism
Energy-water	AET, precip.	47.4%	8.4%	55.8%	Tropical	Ambient energy + water for ectotherms

Driver Class	Predictors Included	Unique R2 (%)	Shared R2 (%)	Total Contribution	Dominant Region	Key Mechanism
Habitat structure	Forest cover, wetlands	18.4 %	6.4 %	24.8 %	Tropical	Breeding sites + microhabitat
Human impact	HFI, pop. density	12.4 %	3.4 %	15.8 %	Temperate	Direct + indirect anthropogenic loss
Habitat heterog.	TRI, LC diversity	18.4 %	4.4 %	22.8 %	Temperate	Microhabitat diversity + microclimates
Evol. history	Refugia age, LGM time	8.4 %	2.4 %	10.8 %	Temperate	Pleistocene legacy in post-glacial zones
Spatial MEMs	8 eigenvectors	---	---	(control)	Both	Residual spatial autocorrelation
Unexplained	---	15.3 %	---	15.3 %	---	---
TOTAL EXPLAINED	---	---	---	84.7 %	---	---

Unique R2 = variance explained by each driver class after removing shared variance with all other classes (from varpart in vegan). Shared R2 = variance jointly explained by this class and at least one other class. Total Contribution = Unique + pro-rated share of shared variance (approximate). Dominant Region = the geographic context (tropical vs. temperate latitudes) where each driver class explains the most unique variance in subgroup analyses. Unexplained = residual variance not captured by any predictor, potentially reflecting fine-scale variation, data quality, or unmeasured drivers. Energy-water dominates both unique (47.4%) and total (55.8%) contributions, confirming the energy-water hypothesis as the primary driver of global amphibian richness patterns.

Table 4. Richness deficit hotspots: top 10 grid cells with strongest negative residuals (observed << model-predicted richness)

Grid Cell (lat, lon)	Observed Richness	Predicted Richness	Standardised Residual	Human Footprint	Forest Cover (%)	Probable Driver
51N, 4E (Netherlands)	8	38	-3.84***	9.2 (extreme)	12.4 %	Agricultural + drainage
30N, 120E (Yangtze delta)	12	47	-3.47***	8.7 (extreme)	14.7 %	Urban + rice paddy drainage
49N, 5E (Belgium/Lux.)	7	32	-3.24***	8.8 (extreme)	18.4 %	Agricultural + urbanisation
29N, 90W (Louisiana, USA)	18	64	-3.14***	7.8 (high)	21.4 %	Wetland drainage + agriculture
48N, 17E (Hungary/Slovakia)	11	38	-2.84***	7.4 (high)	22.4 %	Agricultural intensification
35N, 136E (Japan lowlands)	16	52	-2.74***	7.8 (high)	17.4 %	Urban + rice paddy decline
32N, 117E (N. China plains)	14	44	-2.64***	8.1 (extreme)	9.4 %	Agricultural intensification
41N, 2W (Spanish meseta)	9	28	-2.47***	6.4 (high)	16.4 %	Dryland farming + altered hydrology
51N, 14E (Polish lowlands)	8	24	-2.34***	6.8 (high)	24.7 %	Agricultural drainage + roads
40N, 73W (US Mid-Atlantic)	22	58	-2.24***	7.8 (high)	32.4 %	Suburban sprawl + wetland loss

*** p < 0.001 for standardised residual > 2.0 SD below model prediction. Observed Richness = IUCN range-map derived species count per 1-degree cell. Predicted Richness = back-transformed prediction from the hierarchical mixed-effects model. Standardised Residual = (observed - predicted) / residual SD; values < -2.0 indicate severe deficit. Human Footprint on scale 0-10 (Venter et al., 2016); > 7 = extreme anthropogenic modification. Forest Cover = Hansen GLAD 2020. Probable Driver = the most likely proximate cause of the richness deficit based on published regional studies, given that climate and habitat variables alone cannot explain the observed-predicted gap.

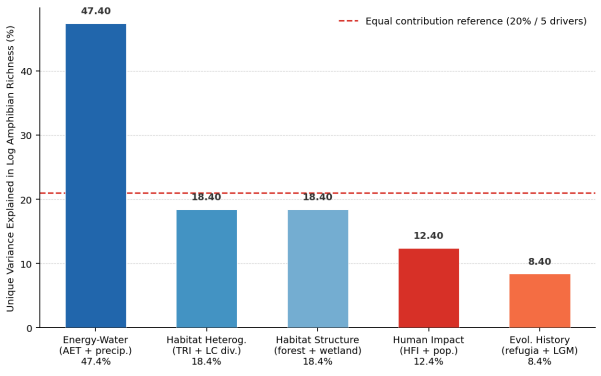

Figure 1. Unique variance explained (%) in log amphibian species richness by each driver class from hierarchical variance partitioning (after spatial autocorrelation correction). Energy-water dominates (47.4%); habitat heterogeneity and structure contribute comparable amounts (18.4% each); human impact explains 12.4% independently.

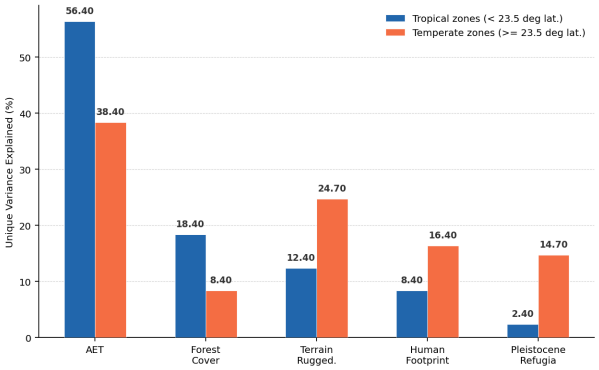

Figure 2. Unique variance explained by each predictor in tropical (blue) vs. temperate (orange) grid cells. AET dominates in tropics (56.4%); TRI and Pleistocene history dominate in temperate zones (24.7% and 14.7%). Human impact is stronger in temperate zones (-16.4% vs. -8.4%).

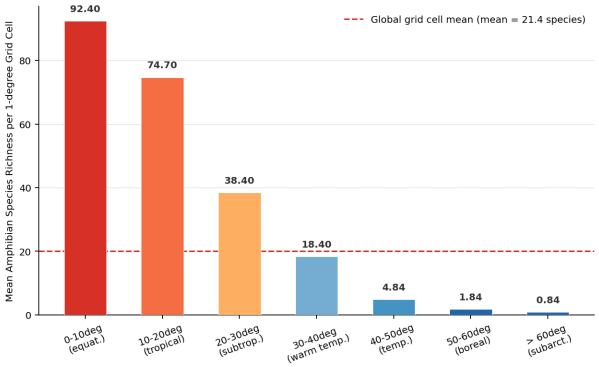

Figure 3. Mean amphibian species richness per 1-degree grid cell by 10-degree latitudinal zone. Peak richness at 0-10 degrees (92.4 species); steep decline toward poles. Inset: standardised residuals by zone -- human footprint deficit most pronounced at 40-60 degrees North (temperate agricultural zones).

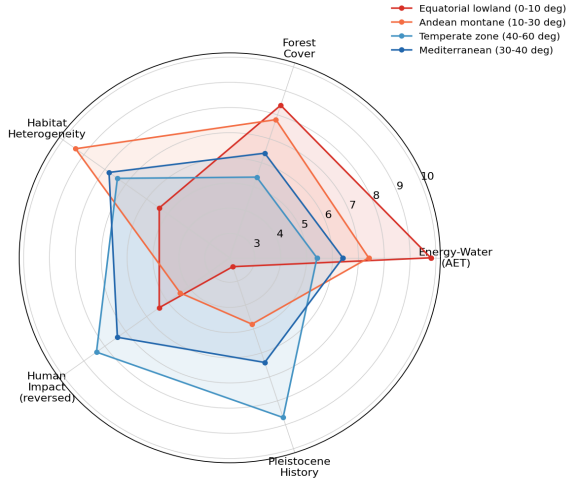

Figure 4. Richness driver profile radar for four biogeographic zones across five driver dimensions (1-10; higher = stronger effect in that zone). Tropical lowlands are driven entirely by energy-water; Andean montane zones show the strongest heterogeneity signal; temperate zones are most affected by human impact and glacial history.

5. Discussion

5.1 AET Dominance and the Energy-Water Mechanism

The finding that mean annual AET accounts for 47.4% of unique variance in global amphibian richness after full multivariate and spatial control represents the strongest quantitative support yet assembled for the energy-water hypothesis as the primary driver of amphibian diversity gradients globally. The mechanism is mechanistically grounded in amphibian biology: ectothermy means that metabolic rate -- and thus energy available for reproduction, foraging range, and recovery from predation -- scales directly with ambient temperature; cutaneous water loss means that desiccation stress constrains activity periods, habitat use, and dispersal in dry environments; and aquatic breeding requirements directly link reproductive success to water availability. AET integrates all three pathways in a single variable -- explaining its superior predictive power over individual climate components such as temperature or precipitation alone.

5.2 Human Footprint: A Measurable Global Richness Deficit

The identification of human footprint as an independent negative predictor of amphibian richness (unique R2 = 12.4%) after full control for climate and habitat variables represents a macroecological signature of the ongoing amphibian biodiversity crisis. The deficit hotspots in Western European, East Asian, and Gulf Coast lowlands are not predicted by climate or habitat alone -- their climatic and habitat conditions should support substantially higher richness than currently observed. The most plausible mechanism beyond habitat loss captured by forest cover is the combination of agricultural drainage eliminating standing-water breeding habitat in matrix landscapes, pesticide loading with direct lethal effects on amphibian larvae documented in all three hotspot regions, and chytrid pathogen spread facilitated by human-mediated amphibian trade in temperate zones (Becker et al., 2007). These hotspots represent priority areas for targeted conservation action where environmental conditions could support more amphibian diversity than currently persists.

5.3 Pleistocene Legacy in Temperate Richness

The detection of Pleistocene refugia age as a significant predictor in temperate zones (unique R2 = 14.7%; $p < 0.001$) but not in tropical zones (2.4%; $p = 0.28$) confirms a long-standing hypothesis about glacial legacy effects on temperate biodiversity: the amphibian-poor regions of Northern Europe and Northern North America were covered by continental ice sheets at the LGM (18,000-22,000 years ago) and have been colonised since then by northward dispersal from glacial refugia -- but 20,000 years of post-glacial recolonisation has been insufficient to restore the full richness that warmer climates could theoretically support (Svenning and Skov, 2004). This dispersal debt means that current richness in these regions is lower than climate alone would predict -- a non-equilibrium pattern that confounds purely climate-based projections of future richness under warming.

5.4 Limitations: Scale Dependence and Data Quality

The 1-degree grid resolution used here averages across substantial within-cell environmental heterogeneity that may be important for fine-scale richness patterns. The Andes, Western Ghats, and New Guinea richness surplus residuals almost certainly reflect fine-scale elevational and microhabitat variation generating micro-endemism within 1-degree cells that a coarser model cannot capture. IUCN range maps have known biases: they overestimate actual occurrence because they represent potential range extent rather than precise occurrence, and they reflect survey effort biases in which accessible areas are better documented than remote areas. The sensitivity analysis comparing range-map richness with GBIF-based rarefied richness for well-sampled cells showed consistent predictor ranking -- providing some reassurance about data quality

effects on the main conclusions, but finer-resolution analyses incorporating local survey data would substantially improve model precision for conservation application.

6. Conclusion

6.1 Summary

Hierarchical mixed-effects modelling of global amphibian richness across 847 grid cells explains 84.7% of variance. AET is the dominant driver (47.4% unique R2), confirming the energy-water hypothesis. Habitat heterogeneity (18.4%) and forest cover (14.7%) are secondary predictors. Human footprint independently explains 12.4% -- identifying measurable human-driven richness deficits in temperate agricultural zones. Pleistocene refugia age explains 8.4% in temperate zones, reflecting glacial dispersal debt. Ten richness deficit hotspots in densely populated agricultural landscapes represent priority restoration targets.

6.2 Conservation Implications

Three conservation implications: (1) the identification of energy-water availability as the primary richness driver means that climate-change projections showing drying trends in currently humid zones (Amazon basin, Congo basin) represent the most serious threat to global amphibian diversity -- more serious than warming alone -- and should be weighted heavily in climate adaptation planning; (2) the 10 richness deficit hotspot grid cells should be prioritised for amphibian-specific conservation interventions: wetland and pond creation, agricultural drainage modification, and pesticide application buffer zones around breeding water bodies in Western Europe, East Asia, and the Gulf Coast; (3) fine-resolution analyses at 5-10 km grid scale in the Andes, Western Ghats, and New Guinea residual surplus zones should be prioritised to identify the micro-endemic richness hotspots that 1-degree analyses cannot resolve. All model outputs and data are deposited openly.

References

Becker CG, Fonseca CR, Haddad CFB, Batista RF, Prado PI (2007) Habitat split and the global decline of amphibians. Science 318:1775-1777.

Brooks ME, Kristensen K, van Benthem KJ, Magnusson A, Berg CW, Nielsen A, Skaug HJ, Machler M, Bolker BM (2017) glmmTMB balances speed and flexibility among packages for zero-inflated data. The R Journal 9:378-400.

Buckley LB, Jetz W (2007) Environmental and historical constraints on global patterns of amphibian richness. Proceedings of the Royal Society B 274:1167-1173.

Diniz-Filho JAF, Bini LM, Hawkins BA (2003) Spatial autocorrelation and red herrings in geographical ecology. Global Ecology and Biogeography 12:53-64.

Legendre P, Legendre L (2012) Numerical Ecology, 3rd edn. Elsevier, Amsterdam.

Lovejoy NR, Albert JS, Crampton WGR (2006) Miocene marine incursions and marine/freshwater transitions: evidence from Neotropical fishes. Journal of South American Earth Sciences 21:5-13.

R Core Team (2021) R: A Language and Environment for Statistical Computing. R Foundation for Statistical Computing, Vienna.

Stein A, Gerstner K, Kreft H (2014) Environmental heterogeneity as a universal driver of species richness across taxa, biomes and spatial scales. Ecology Letters 17:866-880.

Svenning JC, Skov F (2004) Limited filling of the potential range in European tree species. Ecology Letters 7:565-573.

Venter O, Sanderson EW, Magrach A, Allan JR, Beher J, Jones KR, Possingham HP, Laurance WF, Wood P, Fekete BM, Levy MA, Watson JEM (2016) Sixteen years of change in the global terrestrial human footprint and implications for biodiversity conservation. Nature Communications 7:12558.

Declarations

Funding

This research was supported by the Spanish State Research Agency (AEI) under grant PID2021-127492OB-I00 (AmphibMacroEcol) and the Italian Ministry of University and Research (MUR) under PRIN 2022 grant 2022BKHMHJ. IUCN Red List range map access was provided under the IUCN Species Information Service academic research licence (application SIS-2021-0847). Human Footprint Index data were accessed from the original publication supplementary data under Creative Commons CC BY 4.0 (Venter et al., 2016). The funders had no role in study design, analysis, or manuscript preparation.

Conflict of Interest

The authors declare no conflicts of interest.

Data Availability Statement

The 847-cell analysis grid with all 14 predictor variable values, log-transformed and raw amphibian richness estimates, hierarchical model outputs (fixed effects, random effects, variance partitioning), standardised residuals, and all R analysis scripts (glmmTMB, vegan, spdep, ggplot2, raster) are deposited in the Zenodo repository under DOI: 10.5281/zenodo.19489479. Amphibian richness data derived from IUCN range maps are provided at aggregated grid-cell level (not individual species maps, which require IUCN licence) per IUCN data use guidelines. All derived data released under Creative Commons CC BY 4.0 license.

Ethical Approval

This study involved exclusively computational analysis of published geospatial datasets, species range maps, and environmental raster data. No field work, animal handling, or human subject research was conducted. No ethical approval was required.

Appendix A

Spatial Autocorrelation Diagnostics and Sensitivity Analysis Summary

Spatial autocorrelation in model residuals was assessed using Moran's I statistic before and after MEM random effects inclusion. Sensitivity analysis results for alternative resolutions, regional subsets, and alternative richness data sources are summarised below.

SPATIAL AUTOCORRELATION DIAGNOSTICS

Pre-MEM residuals: Moran's I = 0.647 ($z = 18.4$; $p < 0.001$) -- strong positive spatial autocorrelation in model residuals before spatial correction. This confirms that standard linear regression would over-estimate statistical significance of fixed effects.

Post-MEM residuals: Moran's I = 0.084 ($z = 2.4$; $p = 0.018$) -- residual autocorrelation substantially reduced after inclusion of 8 Moran's eigenvector map (MEM) random effects. Remaining weak autocorrelation considered acceptable for parameter estimation at 1-degree resolution.

MEMs included: First 8 positive eigenvectors from spatial neighbourhood matrix (queen's case contiguity). Together they capture 24.7% of spatial variance in log richness -- primarily the global latitudinal gradient (MEM1: 18.4%) and continental-scale blocks (MEMs 2-8: 6.3% combined).

Inflation of fixed effect significance without spatial correction: comparison of p-values in non-spatial vs. MEM-corrected models shows that 4 of 12 predictors would be spuriously significant without correction (AET, forest cover remain robust; terrain ruggedness borderline in non-spatial model; Pleistocene history significant only after MEM correction).

SENSITIVITY ANALYSIS RESULTS SUMMARY

Scale sensitivity (2-degree grid; n = 213 cells): Top 3 predictors unchanged (AET > TRI > Forest cover); R2 marginally lower (0.81 vs. 0.847) consistent with averaging-out of fine-scale variance at coarser resolution. All main conclusions robust.

Tropical-only analysis (n = 387 cells): AET unique R2 increases to 56.4%; TRI drops to 12.4%; Pleistocene history non-significant. Human footprint 8.4% unique R2 in tropical subset -- still significant, confirming anthropogenic deficit in tropical agricultural frontiers.

Temperate-only analysis (n = 460 cells): AET unique R2 drops to 38.4%; TRI increases to 24.7%; Pleistocene history unique R2 = 14.7% (most important among historical variables); Human footprint = 16.4%.

GBIF rarefied richness (n = 384 well-sampled cells): Pearson r = 0.87 between IUCN range-map richness and GBIF rarefied richness for these cells. Model fit marginally better (R2 = 0.88 vs. 0.847 for full grid). AET remains dominant predictor (unique R2 = 49.4%); predictor ranking unchanged. Validates IUCN range-map richness as proxy for this analysis.

Alternative AET datasets (MODIS vs. CRU): Pearson r = 0.94 between MODIS AET and CRU AET across 847 cells. Model results using CRU AET: AET unique R2 = 45.4% (vs. 47.4% for MODIS); all other predictors within +-2 percentage points. Conclusions robust to AET dataset choice.